Published in final edited form as:
Exp Neurol. 2008 June ; 211(2): 539–550. doi:10.1016/j.expneurol.2008.02.031.

Axotomy or compression are required for axonal sprouting following end-to-side neurorrhaphy

Ayato Hayashi, MD, PhD[*], **Christopher Pannucci, MD**[*], **Arash Moradzadeh, MD**[**], **David Kawamura, MD**[*], **Christina Magill, MD**[**], **Daniel A. Hunter, RA**[*], **Alice Y. Tong, MS**[*], **Alexander Parsadanian, PhD**[***], **Susan E. Mackinnon, MD**[*], and **Terence M. Myckatyn, MD**[*]

[*]Division of Plastic and Reconstructive Surgery, Washington University School of Medicine, Campus Box 8238, 660 South Euclid Ave., St. Louis, MO, 63110

[**]Department of Otolaryngology, Washington University School of Medicine

[***]Department of Neurology and Hope Center for Neurological Disorders, Box 8518, Washington University School of Medicine, 660 South Euclid Avenue, St. Louis, MO 63110, USA.

Abstract

End-to-side (ETS) nerve repair remains an area of intense scrutiny for peripheral nerve surgeon-scientists. In this technique, the transected end of an injured nerve, representing the “recipient” is sutured to the side of an uninjured “donor” nerve. Some work suggests that the recipient limb is repopulated with regenerating collateral axonal sprouts from the donor nerve that go on to form functional synapses. Significant, unresolved questions include whether the donor nerve needs to be injured to facilitate regeneration, and whether a single donor neuron is capable of projecting additional axons capable of differentially innervating disparate targets. We serially imaged living transgenic mice (n=66) expressing spectral variants of GFP in various neuronal subsets after undergoing previously described atraumatic, compressive, or epineurotomy forms of ETS repair (n=22 per group). To evaluate the source, and target innervation of these regenerating axons, nerve morphometry and retrograde labeling was further supplemented by confocal microscopy as well as Western blot analysis. Either compression or epineurotomy with inevitable axotomy were required to facilitate axonal regeneration into the recipient limb. Progressively more injurious models were associated with improved recipient nerve reinnervation (epineurotomy: 184±57.6 myelinated axons; compression: 78.9±13.8; atraumatic: 0), increased Schwann cell proliferation (epineurotomy: 72.2% increase; compression: 39% increase) and cAMP response-element binding protein expression at the expense of a net deficit in donor axon counts distal to the repair. These differences were manifest by 150 days, at which point quantitative evidence for pruning was obtained. We conclude that ETS repair relies upon injury to the donor nerve.

Keywords

End-to-side neurorrhaphy; myelin associated glycoprotein; epineurotomy; CREB; transgenic; regeneration

Corresponding author: Terence M. Myckatyn, MD, Assistant Professor, Division of Plastic and Reconstructive Surgery, Washington University School of Medicine, Campus Box 8238, 660 South Euclid Ave., St. Louis, MO, 63110, myckatynt@wudosis.wustl.edu, PHONE: (314) 362-4263, FAX: (314) 362-4536.

Introduction

End-to-side (ETS) nerve repair, also known as terminolateral neurorrhaphy is a microsurgical technique where the distal, or terminal, limb of a transected nerve is reinnervated by coapting it into the side of an intact, donor nerve (Fig. 1). In theory, it would have strong clinical value for reconstructing avulsed or proximally injured peripheral nerves. Unfortunately, since the utility of this technique was revisited (Viterbo, et al. 1992), the ETS literature has become rife with contradictory studies including those investigating the number of axons recruited by this technique, and the functional deficit imposed upon the donor nerve (Cederna, et al. 2001). Some have suggested that collateral axonal sprouts repopulate the terminal limb without axotomy, attributing this spontaneous phenomenon to neurotrophic influences (Caplan, et al. 1999,Thanos, et al. 2001). Others suggest that an epineurotomy or perineurotomy, exposing but not injuring donor axons facilitates spontaneous collateral sprouting (Bertelli, et al. 1996). Others show that regenerative sprouting induced by a deliberate axotomy is required to induce some terminal sprouts to regenerate down the recipient pathway rather than the original donor nerve pathway (Brenner, et al. 2007).

In one study, for example, an atraumatic sleeve repair technique without axotomy was compared to an epineurotomy, and found to be sufficient for stimulating axonal sprouting into the terminal limb (Hayashi, et al. 2004). This study suggested that axons could cross intact epineurium and that multiple projections from the same neuron would differentially innervate more than one target (Hess, et al. 2005). Developmental studies, however, have shown that although a single neuron can initially extend numerous axonal projections that differentially respond to local guidance cues (Dickson 2002, Liu and Halloran 2005), one-to-one relationships between neurons and motor units are established after synapse elimination (Bishop, et al. 2004, Keller-Peck, et al. 2001).

In the present study we hypothesized that axonal injury due either to axotomy or compression was necessary to induce sprouting following ETS nerve repair. To test this hypothesis, we performed quantitative serial *in vivo* imaging in XFP mice (Feng, et al. 2000), and corroborated our findings with assays for motor and sensory reinnervation. Assays for myelination, and cAMP regulatory element binding (CREB) protein expression, a transcription factor whose upregulation may be instrumental in overcoming the inhibitory influences of myelin-associated glycoprotein (MAG) on nerve regeneration were also evaluated (Gao, et al. 2004). We compared a repair with epineurotomy to an atraumatic sleeve repair with and without proximal compression since previous work suggests that compression upregulates sprouting of small diameter unmyelinated axons (Mackinnon, et al. 1986). We suspected that the success of ETS repair would be inversely proportional to the degree of donor nerve injury. Resolution of this debate is highly significant since ETS nerve repair has already found its way into clinical practice for reconstruction of an assortment of peripheral nerve injuries (Amr and Moharram 2005, Mennen 2003, Mennen, et al. 2003).

Materials and Methods

Mice

To specifically track and quantify the course of a few motor axons following ETS nerve repair, we used homozygous mThy1-GFP(S) mice (n=33), initially developed by Dr. J. Sanes and colleagues (Harvard University, Cambridge, MA). From the original description, ≤10% of motor axons, but no sensory axons are labeled in this line (Feng, et al. 2000), although we did corroborate a subsequent report that one occasion, 1–2 sensory axons are also labeled (Misgeld, et al. 2007). Homozygous mThy1-YFP(16) mice (Jackson Laboratories, Bar Harbor, ME) were used to track the course of all motor and sensory axons following ETS nerve repair, evaluate

cutaneous and motor endplate reinnervation, and for immunohistochemistry (n=33). C57BL/6J mice (Jackson Laboratories) were used for Western blot analysis where fluorescent imaging was not required (n=9). All experiments were performed in accordance with protocols approved by the Division of Comparative Medicine at the Washington University School of Medicine.

Surgical Model

The femoral nerve functioned as the donor nerve, and was used to reconstruct a transected sciatic nerve (Fig. 2A). First, mice were anesthetized with subcutaneous injections of medetomidine and ketamine and the right median nerve exposed. The median nerve was proximally transected in the axilla, the skin closed with 6-0 nylon, and mice recovered with antisedan on a warming pad. Ten days later, the median nerve was re-exposed under anesthesia and distally transected to provide a 5 mm long fluorescence-naïve predegenerated autograft. The sciatic nerve was exposed through a skin incision 1 mm parallel and posterior to the femur. The sciatic nerve was transected 5 mm proximal to its trifurcation and the proximal cut end was brought to the inguinal region through a tunnel created between the quadriceps femoris and the semimembranosus muscles. The mice were then repositioned supine and the ipsilateral common femoral nerve was exposed through a groin incision. The proximal median nerve graft was sutured ETS to the common femoral nerve, and the distal end of the graft sutured end-to-end to the transected distal sciatic nerve. The purpose of the graft was twofold. It facilitated a tension-free repair, and enabled constitutively labeled axons to be immediately tracked into an autograft made fluorescence-naïve with predegeneration (Fig. 2B). Muscle was closed with 8-0 vicryl, skin closed with 6-0 nylon sutures, and mice recovered as above.

Three different ETS repair techniques were compared, and were performed by the first author (A.H.) who originally described the sleeve repairs (Hayashi, et al. 2004). In the “atraumatic” group (Fig. 2C1&2), the median nerve graft was slit 3 mm, and the resulting two sleeves wrapped around the donor femoral nerve. This construct was secured to the femoral nerve by suturing the sleeves to one another on the other side of the donor femoral nerve with 11-0 sutures without placing any sutures in the femoral nerve itself. In the “compression” group (Fig. 2D1&2), the atraumatic sleeve technique was repeated, but a silicone wrap (0.5 mm internal diameter) was placed around the common femoral nerve 1 mm proximal to the ETS coaptation and snugly secured to itself with 11-0 sutures. In the “epineurotomy” group (Fig. 2E1&2), microscissors were used to slit the femoral nerve epineurium, and a few axons were inevitably injured as visualized with a fluorescent dissecting microscope (SMZ 1500, Nikon Instruments Inc, Melville, NY). The median nerve graft was then sutured with four 11-0 microsutures to capture axons from the femoral nerve.

Serial In Vivo Imaging

In vivo imaging of femoral nerve fibers regenerating through the ETS repair was performed in anesthetized, transgenic mice at the time of reconstruction, at 10 and 15 days, and every month to 5 months using either an Olympus MVX-10 single-zoom optical path (0.63x/0.15 N.A.; 2x/0.5 N.A) fluorescent microscope (Olympus Corporation, Japan) equipped with a cooled Hamamatsu ORCA-ER CCD (Hamamatsu City, Japan) or a Nikon SMZ-1500 fluorescent dissecting microscope (1x/.25 N.A.) equipped with a CoolSNAP-ES monochromatic CCD (Photometrics, Tucson, AZ). To calibrate the images, MetaMorph v 7.1 software (Universal Imaging Corporation, Downingtown, PA) correlated pixels from digitized images to actual distance based on the objective utilized. For mThy1-GFP(S) mice, the number of GFP-labeled axons entering the ETS repair were counted, and the net distance they regenerated recorded. Box plots were used to show both the mean and median distance that labeled axons regenerated into the ETS repair over time. The sural nerve branch of the sciatic nerve, whose territory is superiorly defined by the inferior edge of the lateral hamstring and extends inferior to the lateral

ankle and foot was transcutaneously imaged following depilation, as previously described for the saphenous nerve (Pan, et al. 2003). The territory was imaged prior to injury, and at 3 and 5 months to evaluate whether any fibers from the femoral nerve regenerated through the ETS repair and into the sural sensory branch (Olympus MVX-10).

Immunohistochemistry

Mice were deeply anesthetized and then perfused with heparinized 0.01 M phosphate buffered saline (PBS) and 4% paraformaldehyde. The femoral nerve, median nerve graft, and distal transected sciatic nerve and extensor digitorum longus (EDL) muscles were harvested and postfixed for 30 minutes. Nerve and muscle specimens were evaluated as whole mounts under confocal microscopy, after which designated specimens were frozen in OCT compound at −80 °C for immunolabeling. 15 μm sections were blocked with 5% normal goat serum and diluted with 0.3% Triton-X in PBS for one hour. Nuclei were labeled with DAPI (Invitrogen, Eugene, OR), Schwann cells (SCs) with rabbit polyclonal anti-S100 antibody (DAKO, Carpinteria, CA), myelin basic protein (MBP) with rabbit polyclonal anti-MBP antibody (CHEMICON, Temecula, CA), and phosphorylated CREB (pCREB) with rabbit monoclonal anti-phospho-CREB (Ser-133) (Cell signaling, Danvers, MA) all diluted 1:100 and incubated overnight at 4°C. Cy5-conjugated goat anti-rabbit antibody and Cy3-conjugated donkey anti-rabbit antibody (Jackson ImmunoResearch, West Grove, PA) were diluted 1:500 and used to label anti-S100 and anti-phospho CREB antibodies. Sections were evaluated with confocal microscopy using an Olympus FV1000 spectral scanning microscope with 20x, 40x, and 60x (oil) objectives with numerical apertures of 0.75, 0.9, and 1.42 (Olympus Corporation, Japan). We used a multi-line 458, 488, and 515 nm laser as well as 405 nm, 561 nm, and 633 nm lasers.

Motor Endplate Evaluation

The harvested EDL muscles of mThy1-YFP(16) mice were used to measure the percentage of reinnervated motor endplates originally innervated by a peroneal branch of the transected sciatic nerve. These reinnervating motor axons originated from the femoral nerve through the ETS repair. 150 days after ETS repair, whole EDL specimens were soaked for 30 minutes in a 1:100 solution of Alexa 594-conjugated alpha-bungarotoxin (BTX; Molecular Probes, Eugene, OR). Labeled specimens were surveyed under fluorescent microscopy and regions containing endplates imaged with the confocal microscope with a 40x oil (1.3 N.A) objective using 515 and 561 nm lasers (Magill, et al. 2007). Flattened Z-series stacks from 100 randomly sampled areas (100 μm^2) occupied by motor endplates (≥300 endplates per group) were evaluated and the percentage reinnervated calculated.

Histomorphometry, Non-Biased Stereology, and Quantitative Immunohistochemistry

Donor nerves 5 mm proximal and distal to the ETS repair as well as the sciatic nerve 5 mm distal to the median nerve graft were harvested 5 months after surgery (Fig. 6A). Specimens from 6 mice per group were preserved in 3% glutaraldehyde, postfixed in 1% osmium tetroxide, dehydrated in gradations of ethanol and embedded in Araldite 502 resin, and 1 μm sections stained with 1% toluidine blue. Histomorphometry of the entire nerve cross section was performed with quantitative bit-plane analysis aided by Leco IA32 software (Leco, St. Joseph, Michigan) software as we have previously described (Hunter, et al. 2007). For electron microscopy, 90 nm sections of nerve grafts were sectioned with an LKB III microtome (Bromma, Sweden) and stained with uranyl acetate and lead citrate. For each group, 10 ultramicrographs were taken with a Zeiss 902 electron microscope (Zeiss Instruments, Chicago, IL) at 4360x magnification, scanned at 400 dots per inch resolution (Epson Perfection 4870 scanner) and evaluated with MicroBright Field Stereo Investigator software (MBF Bioscience StereoInvestigator version 7.0, Williston, Vermont). Using the fractionator technique, a four ray 2D vertical nucleator probe was used to evaluate the number and area of

unmyelinated axons in the scanned micrographs (Hayashi, et al. 2007). A sampling frame grid of 225 μm^2 was selected by the software to minimize sampling error.

Quantification of DAPI and pCREB labeling was performed using greyscale thresholding with Leco software set at a minimum value of 45 (1–255 pixel value range) as previously described (Hayashi, et al. 2007). All DAPI-labeled nuclei detected with the 405 nm laser, and pCREB (+)ve nuclei detected with the 561 nm laser that were visible with this degree of thresholding were counted (minimum 500 nuclei per group).

Retrograde Labeling

Five months after ETS repair, 4 μl of Fast Blue (Polysciences, Warrington, PN) was injected as 4 separate 1 μl aliquots into the deep surface of the lateral head of the gastrocnemius muscle under general anesthesia. Six days later, mice were deeply anesthetized, perfused, and the spinal cord harvested by performing laminectomies at the L2–L4 level. Spinal cords were placed in 10% sucrose with 0.1 *M* Sorenson's phosphate buffer, frozen in OTC compound, and sectioned (40 μm). A blinded observer counted the spinal cord sections using an optical fractionator with a 75,000 μm^2 sampling grid (MicroBright Field Stereo Investigator) and motorized stage. Means of the sum total of labeled, in-focus motor neurons from the entire depth of each spinal cord per experimental group were reported.

Western Blot Analysis

Three donor nerves per group were harvested and divided into 5 mm segments immediately proximal and distal to the coaptation 3 weeks after ETS repair. Segments were homogenized in lysis buffer (50 mM Tris pH 7.4, 150 mM Na Cl, 1% NP40, 10% Glycerol, 1mM EGTA, protease inhibitor cocktail, and 1 mM sodium orthovanadate) and centrifuged with supernatants retained for analysis. The samples were mixed with SDS-PAGE sample buffer (Bio-Rad, Hercules, CA) and boiled for 3 min after which 10 μg of protein was loaded and resolved in 4% to 12% SDS-PAGE gels (Invitrogen, Carlsbad, CA). Resolved proteins were transferred to nitrocellulose membranes (Bio-Rad, Hercules, CA), incubated with 5% bovine serum albumin (Sigma, St. Louis, MO) and TBS-Tween buffer, and primary antibodies added. The next day, immunoblots were incubated with secondary antibody conjugated to HRP [Goat anti-rabbit (1:5,000 dilution; Santa Cruz, Santa Cruz, CA)] in blocking solution. An hour later, immune complexes were detected by enhanced chemiluminescence (LumiGLO, Cell signaling, Danvers, MA). Protein loading was normalized to GAPDH signal. Immunoreactive band intensity was quantified by assessing scanned autoradiographs with Gel-pro analyzer version 3.0 (Media Cybernetics, Bethesda, MD). Primary antibodies were anti-myelin-associated glycoprotein, and anti-GAPDH (both rabbit polyclonal; Santa Cruz, Santa Cruz, CA) diluted 1:500.

Statistical Analysis

Statistical analyses were performed in Statistica (Version 7.1, StatSoft, Tulsa, OK). Significant differences within endplate innervation, morphometric, stereologic, and Western blot data sets were identified using a one-way analysis of variance, and further evaluated using *post hoc* Scheffe or Student-Newman-Keuls tests. Results were considered significant when $p<0.05$. A frequency distribution of the morphometric data based on fiber diameter or area was generated in Prism (Version 4.0, GraphPad Software Inc.).

Results

Visualization of Axonal Sprouting in Transgenic Mice

When the atraumatic technique was employed in mThy1-YFP(16) mice (Fig. 3A–C) where all peripheral axons are labeled (Feng, et al. 2000), faint YFP labeling was noted in 2 of 6 atraumatic ETS repairs suggesting the presence of a few axons by 60 days in one mouse, 90 days in another, but not the remaining 4. When proximal compression was added to atraumatic ETS repair (Fig. 4A), there was clear evidence of axonal sprouting by 60 days (Fig 4B) in all (n=8) serially imaged mThy1-YFP(16) mice. By 90 days, confocal imaging demonstrated regenerative sprouting both proximal and distal to the ETS repair (Fig. 4C1). Sprouts were noted both proximal (Fig. 4C2), and distal (Fig. 4C3) to the compressive cuff, and a few regenerative sprouts were also noted in the previously fluorescent naïve recipient limb (Fig. 4C4) and in the donor nerve distal to the ETS repair (Fig. 4C5). By 150 days, sprouting was robust into the recipient nerve graft (Fig. 4D1), but sprouting proximal (Fig. 4D2) and distal to the graft was absent, but present at the ETS repair site (Fig. 4D3). Epineurotomy resulted in the most rapid and robust regeneration. Axons were clearly disrupted by 10 days (Fig. 5A). mThy1-GFP(S) mice clearly demonstrated more axons proximal to, than distal from, the repair. By 150 days, many axons were noted in the recipient limb, and proportionately fewer axons were still noted in the distal than proximal donor nerve (Fig. 5B).

We used mThy1-GFP(S) mice to measure the course of individual axons into the median nerve graft and eventually the sciatic nerve. The maximal regenerative distance was 3.1 to 3.5 cm before muscle targets were approached obscuring visualization. Shown in Fig. 5C, no labeled axons entered the atraumatic repairs (n=6), while the earliest evidence of axons entering the repair in the compression group ranged from 15–60 days (n=8), and was much more rapid (≤10 days) with epineurotomy (n=8). Reported as box plots (Fig. 5D), we found that the *median* (50^{th} %ile) axon length was 1.6 cm in the compression group and 3.0 cm in the epineurotomy group (Fig. 5E), indicating that a much higher percentage of axons reached their endplate targets by 150 days following epineurotomy (n=8). Furthermore, the *mean* axon length actually began to drop in the epineurotomy group but not the compression group. This was explained by the fact that as some regenerated axons reached their targets, the other sprouts were pruned, becoming successively shorter thereby creating a bimodal length distribution and reducing the mean length of axons in the ETS repair overall.

Histomorphometry and Non-Biased Stereology of Nerve Regeneration

The total number of donor femoral nerve myelinated axons proximal to ETS repair was 546.6 ±15.3 and did not differ significantly between groups at any fiber diameter (Fig. 6A&B). Sciatic nerve sections were evaluated 5 mm distal to the median nerve graft to evaluate distally regenerated myelinated axons that had traversed the ETS nerve repair (Fig. 6A). By 150 days, there were significantly more myelinated axons within the epineurotomy ETS repair technique overall (184.0±57.6) and at all fiber diameters except those ≤1 μm ($p<0.01$; Fig. 6C). Corroborating our live and confocal imaging data, there were no myelinated axons detected with the atraumatic ETS technique but a few with the compressive technique (78.9 ± 13.8). Distal to the repair (Fig. 6D), the donor femoral nerve had significantly fewer axons by 150 days ($p<0.05$) following the epineurotomy repair (381.7±48.3). This trend was also observed with the compressive technique (515.4±51.2) but did not achieve statistical significance relative to the atraumatic technique (554.3±23.3). The sum total of myelinated axons in the distal femoral nerve donor and sciatic nerve reconstructed with ETS repair were not significantly different from the proximal donor nerve.

Unmyelinated axon densities stratified by fiber area (Fig. 6E), and Remak bundle ratios (Fig. 6F) were calculated in the sciatic nerve reconstructed with ETS repair. No unmyelinated axons

associated with SCs or a double basement membrane were noted with atraumatic repair although 0–4 atrophic axons (2.3± 3.1) were noted in a few sections (Fig. 6G). There were significantly more unmyelinated axons with compression (Fig, 6H; 101.4±23.2) and epineurotomy repair (Fig. 6I; 55.1±19.7), particularly with fiber areas ≤2 μm^2 ($p<0.05$). Remak bundles tended to be larger with the compression repair, with up to 5 unmyelinated axons per SC (Fig. 6F). Qualitatively, the distal donor nerve appeared uninjured with atraumatic repair, and possessed tightly packed myelinated and unmyelinated axons with little debris (Fig. 6J). With compressive repair, extremely large Remak bundles, with up to 47 unmyelinated axons/SC were noted (Fig. 6K) while some neural debris and less densely clustered axons were noted in the distal donor nerve with the epineurotomy technique (Fig. 6L).

Motor Endplate Reinnervation

To quantify the number of motor axons originating from the common femoral nerve but innervating sciatic nerve targets, we assessed reinnervation of the EDL (Fig. 7A–E). The peroneal branch of the sciatic nerve normally innervates this muscle. Uninjured control mThy1-YFP(16) mice demonstrated 100% innervation of EDL motor endplates (Fig. 7A). Transected sciatic nerves repaired with atrauamtic ETS repair from the femoral nerve failed to demonstrate any endplate reinnervation at 150 days (Fig. 7B&E) while the addition of a proximal compressive cuff modestly, but statistically significantly increased endplate reinnervation ($p<0.05$; Fig. 7C&E). ETS repair with epineurotomy resulted in innervation of 87±14% of endplates at 150 days (Fig. 7D&E), which was significantly higher than any treatment group ($p<0.0001$).

Retrograde Labeling of Ventral Motor Neurons

To further confirm that femoral motor axons were reinnervating sciatic nerve branches, the retrograde tracer Fast Blue was injected into the lateral head of the gastrocnemius muscle. Fast blue-labeled ventral MNs were counted at the L2-L4 level of the spinal cord (femoral nerve level), but not at the S1-S2 level from where tibial nerve axons that normally innervate the gastrocnemius arise. The atraumatic technique resulted in minimal retrograde labeling of femoral nerve-derived axons at the spinal cord level (Fig. 7F&I), significantly more with application of proximal compression ($p<0.05$; Fig. 7G&I), and the most with epineurotomy ($p<0.0001$; Fig. 7H&I).

Transcutaneous Imaging of Sural Nerve

We specifically imaged the sural branch of the sciatic nerve to confirm that sensory axons derived from the femoral nerve would repopulate the transected sciatic nerve via the ETS repair (n=4 per group). The sural nerve territory could be imaged transcutaneously from the inferior edge of the hamstring attachment at the knee to the lateral edge of the dorsal foot skin (Fig. 8A). Sciatic nerve transection led to complete loss of constitutive fluorescent labeling of the sural nerve as well as branches of the peroneal and tibial nerves. During the 150 day study, no reinnervation of the sural nerve territory (or any other sciatic nerve derived cutaneous branch) was noted with atraumatic ETS repair under low (≤12.6x) magnification (Fig. 8B1). However, in one of four mice, a few axons were seen at 50x magnification within the superficial peroneal nerve territory (Fig. 8B2). Scant reinnervation of the superficial peroneal but not sural nerve distribution was also noted with transcutaneous imaging of the proximal compression group (Fig. 8C). Restoration of the pre-injury pattern of sural nerve territory innervation was only appreciated with epineurotomy ETS repair (Fig. 8D).

Myelination and CREB Phosphorylation

We identified a statistically significant reduction in MAG expression ($p<0.05$) 3 weeks after repair in the 5 mm segment of donor femoral nerve immediately distal to the ETS repair with

the compression technique (Fig. 9A). Increasingly traumatic ETS repairs correlated with an absolute increase in cellularity and CREB phosphorylation measured by quantification of DAPI and pCREB labeling (Fig. 9B). Relative to the atraumatic technique, cellularity was increased 39% with compression and 72.2% with epineurotomy distal to the ETS repair. Strong pCREB labeling was noted in 70.3% of nuclei in the atraumatic group, but was significantly higher ($p<0.01$) in the compression (95.8%), and epineurotomy (93%) groups. Essentially all pCREB expression colocalized to DAPI-labeled nuclei (Fig. 9C1), located in SCs (Fig. 9C2). Even after compression (Fig. 9D) or epineurotomy (Fig. 9E), pCREB expression remained confined to SCs and not at detectable levels in the cytoplasm of axons.

Discussion

ETS nerve repair is a “puzzling concept” in peripheral nerve reconstruction that “has attracted very little attention from basic neuroscientists” and merits investigation (Geuna, et al. 2006). We demonstrate that donor nerve injury is a prerequisite for clinically-relevant nerve regeneration through ETS nerve repair and occurs coincident with the local upregulation of CREB phosphorylation, and downregulation of MAG expression. While a few latent sensory fibers were intermittently noted, ETS repair posing no traumatic injury to the donor nerve failed to induce functionally significant nerve regeneration. Modification of this atraumatic repair with a proximally located compressive cuff induced a modest degree of regeneration and CREB phosphorylation that was unlikely to be of functional significance.

While most investigators believe that an epi- or perineurotomy is required for axons to sprout through an ETS nerve repair (Bertelli, et al. 1996, Noah, et al. 1997), others suggest that effective sensory axonal sprouting into the ETS repair occurs in the absence of any donor nerve injury. In this aforementioned study, a silicone Y-chamber that secured the donor and recipient limbs to one another facilitated sensory sprouting as attributed to the invasion of donor nerve epineurium with SCs (Matsumoto, et al. 1999). Our data suggests that placement of a compressive silicone cuff proximal to the atraumatic ETS repair downregulates MAG expression distally at 3 weeks, with regeneration into the recipient nerve despite an atraumatic repair. Recognizing that extrinsic nerve compression can increase small diameter unmyelinated axon counts (Mackinnon, et al. 1986), it is conceivable that nerves invested by a compressive silicone Y-chamber sprouted unmyelinated sensory axons.

MAG is a known inhibitor of regeneration in the spinal cord (Filbin 1995, Gao, et al. 2004), but is also implicated in the inhibition of peripheral nerve regeneration (Schafer, et al. 1996). Stimulus-induced activation of the transcription factor CREB through phosphorylation of its serine residues can overcome MAG-mediated inhibition of regeneration (Gao, et al. 2004, Lonze and Ginty 2002). We noted pCREB was upregulated in SC nuclei following both the compressive and epineurotomy forms of ETS nerve repair. CREB phosphorylation may also occur downstream from NCAM-dependent autocrine GDNF-mediated signaling in SCs thus contributing to the SC proliferation observed in the compression and epineurotomy models (Iwase, et al. 2005). pCREB was not colocalized to axons, but nuclear CREB phosphorylation secondary to long-range signaling through retrograde shuttling of receptor-ligand complexes was not evaluated (Riccio, et al. 1997, Watson, et al. 2001).

Interestingly, evidence for delayed, scant ETS graft reinnervation was noted in 2 of the 6 atraumatic repairs evaluated with live fluorescent imaging. Electron microscopy demonstrated a few atrophic, small, unmyelinated axons, not associated with SCs or double basement membranes at 150 days. This static imaging may have explained the presence of YFP in some of the serially imaged atraumatic repairs. Magnified transcutaneous imaging did show a few YFP labeled axons within the superficial peroneal nerve territory by 150 days in one mouse. While these few axons may have represented sprouts through the ETS repair, we could not

clearly discern their origin with transcutaneous imaging. Collateral arbors may have also sprouted from the adjacent saphenous nerve territory to reduce the size of the denervated territory, a phenomenon that is noted clinically with the harvest of sensory nerve grafts (Myckatyn and Mackinnon 2003, Myckatyn and Mackinnon 2004).

Another ETS debate issue focuses on whether a “donor” neuron can maintain and differentially regulate additional peripheral synapses arising from new axonal projections. This is an issue whether axons regenerate into the recipient limb as collateral sprouts in response to diffusible factors (Lundborg, et al. 1994), or as regenerative sprouts in response to injury. Our data showed that axons rapidly regenerated into the ETS repair following epineurotomy, and by 60 days reached motor targets ~3.1 cm away (median length 2.3 cm). However, by 150 days, pruning may have occurred whereby median axon length increased to 3.0 cm, while the mean decreased to 1.9±0.2 cm. So, while median axon length approached the length of mature synapse-forming axons (~3.1 cm), daughter axons whose counterparts made functional synapses may have been pruned back, contributing to a lower mean length. Subsequent morphometric analysis demonstrated a net deficit of myelinated axons distal to the repair site that was proportional to the number of axons repopulating the terminal limb of the ETS repair at 150 days. This supported the presence of pruning whereby a single neuron will ultimately project to only one target. We also found a disproportionately high number of unmyelinated axons in the recipient limb and unusually large Remak bundles 150 days after compression ETS repair (Taveggia, et al. 2005). Regenerating units that have failed to reinnervate their targets, and many subtypes of mature sensory axons are unmyelinated. In light of poor cutaneous reinnervation and incomplete pruning, the disproportionately high number of unmyelinated fibers regenerating into the recipient limb following compressive repair was likely the result of a preponderance of unmatched axons at 150 days.

The most direct evidence for pruning occurs during development where axons retract from previously innervated motor endplates (Keller-Peck, et al. 2001) probably by shedding “axosomes” that are morphologically discrete from the products of Wallerian degeneration (Bishop, et al. 2004). Following traumatic injury, motor endplates are initially polyneuronally innervated before reestablishing a mononeuronal relationship (Gillingwater and Ribchester 2003). In these examples, however, the peripheral target is multiply-innervated by projections from a single axon. During development, axons from multiple neurons compete to maintain synapses with motor endplates (Keller-Peck, et al. 2001), while after axotomy, multiple terminal branches from the same axon project to the same endplate (Magill, et al. 2007). In the case of ETS repair, however, it is the neuron that has to innervate multiple discrete motor units or other peripheral targets to avoid creating a donor nerve deficit.

The plasticity of motor units following motor nerve injury (Rafuse and Gordon 1996, Rafuse and Gordon 1996), and the ability of terminal collateral sprouts to innervate adjacent denervated territories (Dengler, et al. 1989) may explain the absence of a functional donor deficit with ETS nerve repair. In the cat triceps muscle, injured terminal branches from viable axons can reinnervate 5–8 times their normal complement of endplates, dramatically increasing motor unit size, and accounting for minimal functional deficits despite significant donor nerve injury (Rafuse and Gordon 1996, Rafuse and Gordon 1996). This may explain why significant force deficits are resolved when axon counts are not restored (Cederna, et al. 2001, Cederna, et al. 2000). It is important, however to distinguish between the terminal arbors of a single axon, and the axonal projections of a single neuron particularly since these discrete compartments possess unique regulatory and neurodegenerative responses to injury (Gillingwater and Ribchester 2001, Gillingwater and Ribchester 2003). Axonal sprouting - a distinct entity from terminal sprouting (Keller-Peck, et al. 2001) - would be required for a single neuron to differentially assume the control of multiple peripheral targets originally regulated by multiple neurons.

Quantitative evaluation of motor endplate reinnervation and transcutaneous imaging of the sural nerve territory coupled with retrograde labeling confirmed that terminal axons derived from the femoral nerve reinnervated sciatic nerve targets. Consistent with our morphometry, target reinnervation was maximized by epineurotomy. Interestingly, epineurotomy resulted in an unexpectedly high degree of EDL motor endplate reinnervation (87±14%) particularly since the femoral nerve is derived from a smaller motor neuron pool than the sciatic. This discrepancy may have been partially due to incomplete labeling of endplates relative to constitutively-labeled axons. Also, some endplates were likely lost to dismantling of the postsynaptic apparatus after 150 days of denervation (Culican, et al. 1998), thereby increasing the proportion of reinnervated endplates from the few that remained. Finally, since motor units are highly plastic, increased arborization of the remaining nerve terminals may have also contributed to a higher percentage of motor endplate reinnervation (Boyd and Gordon 2003, Rafuse and Gordon 1996, Rafuse and Gordon 1996).

In summary, our data suggest that a donor nerve must be subjected to axotomy or a compressive stimulus for clinically relevant and timely regeneration to occur through an ETS repair. Atraumatic ETS repair, may produce modest sensory collateral sprouting but it appears to be delayed and insufficient to be of clinical consequence. The more injurious form of repair, represented here by epineurotomy with inadvertent axotomy, effectively induced early regenerative sprouting into the terminal limb and robust motor endplate and cutaneous reinnervation at the expense of a measurable donor nerve deficit. We were unable to measure the functional relevance of this deficit herein since a method for measuring sciatic nerve recovery in the setting of donor femoral nerve injury is, to our knowledge, unavailable (Nichols, et al. 2005). However, the inverse relationship we noted between donor and recipient axon counts at 150 days suggests that a single neuron will ultimately support a single motor unit or sensory territory but may sprout multiple terminal arbors within that territory. These findings, do not preclude the clinical application of ETS repair in cases where only a few axons are required to innervate a small muscle or cutaneous territory. A small donor deficit, particularly in the context of highly plastic terminal axonal branches, may be acceptable. For the reconstruction of large nerves, however, more mainstream options like nerve grafts or transfers should be thoroughly explored and ETS repair reserved for instances where no other options are available (Dvali and Mackinnon 2003).

Acknowledgements

The authors are extremely grateful to Mr. S. Tuffaha for assistance with Western analysis, and Ms. J. Luciano for maintaining, breeding, and genotyping the transgenic mouse lines. This work was funded by the National Institute of Health 5RO1NS051706-02 grant (S.E.M.). It was also funded by fellowship funding from the American College of Surgeons C. James Carrico Faculty Research Fellowship (T.M.M.) and the American Association of Plastic Surgeons John E. Hoopes Academic Scholarship (T.M.M.) The authors also recognize the Barnes-Jewish Foundation for confocal microscopy equipment support (S.E.M. and T.M.M.).

REFERENCES

1. Amr SM, Moharram AN. Repair of brachial plexus lesions by end-to-side side-to-side grafting neurorrhaphy: experience based on 11 cases. Microsurgery 2005;25:126–146. [PubMed: 15389968]
2. Bertelli JA, Soares dos Santos AR, Calixto JB. Is axonal sprouting able to traverse the conjunctival layers of the peripheral nerve? A behavioral, motor, and sensory study of end-to-side nerve anastomosis. Journal of Reconstructive Microsurgery 1996;12:559–563. [PubMed: 8951126]
3. Bishop DL, Misgeld T, Walsh MK, Gan WB, Lichtman JW. Axon branch removal at developing synapses by axosome shedding. Neuron 2004;44:651–661. [PubMed: 15541313]
4. Boyd JG, Gordon T. Neurotrophic factors and their receptors in axonal regeneration and functional recovery after peripheral nerve injury. Mol Neurobiol 2003;27:277–324. [PubMed: 12845152]

5. Brenner MJ, Dvali L, Hunter DA, Myckatyn TM, Mackinnon SE. Motor neuron regeneration through end-to-side repairs is a function of donor nerve axotomy. Plast Reconstr Surg 2007;120:215–223. [PubMed: 17572566]
6. Caplan J, Tiangco DA, Terzis JK. Effects of IGF-II in a new end-to-side model. J Reconstr Microsurg 1999;15:351–358. [PubMed: 10445516]
7. Cederna PS, Kalliainen LK, Urbanchek MG, Rovak JM, Kuzon WM Jr. "Donor" muscle structure and function after end-to-side neurorrhaphy. Plast Reconstr Surg 2001;107:789–796. [PubMed: 11310430]
8. Cederna PS, Youssef MK, Asato H, Urbanchek MG, Kuzon WM Jr. Skeletal muscle reinnervation by reduced axonal numbers results in whole muscle force deficits. Plast Reconstr Surg 2000;105:2003–2009. [PubMed: 10839398]discussion 2010-2001
9. Culican SM, Nelson CC, Lichtman JW. Axon withdrawal during synapse elimination at the neuromuscular junction is accompanied by disassembly of the postsynaptic specialization and withdrawal of Schwann cell processes. J Neurosci 1998;18:4953–4965. [PubMed: 9634561]
10. Dengler R, Konstanzer A, Hesse S, Schubert M, Wolf W. Collateral nerve sprouting and twitch forces of single motor units in conditions with partial denervation in man. Neurosci Lett 1989;97:118–122. [PubMed: 2918993]
11. Dickson BJ. Molecular mechanisms of axon guidance. Science 2002;298:1959–1964. [PubMed: 12471249]
12. Dvali L, Mackinnon S. Nerve repair, grafting, and nerve transfers. Clin Plast Surg 2003;30:203–221. [PubMed: 12737353]
13. Feng G, Mellor RH, Bernstein M, Keller-Peck C, Nguyen QT, Wallace M, Nerbonne JM, Lichtman JW, Sanes JR. Imaging neuronal subsets in transgenic mice expressing multiple spectral variants of GFP. Neuron 2000;28:41–51. [PubMed: 11086982]
14. Filbin MT. Myelin-associated glycoprotein: a role in myelination and in the inhibition of axonal regeneration? Curr Opin Neurobiol 1995;5:588–595. [PubMed: 8580710]
15. Gao Y, Deng K, Hou J, Bryson JB, Barco A, Nikulina E, Spencer T, Mellado W, Kandel ER, Filbin MT. Activated CREB is sufficient to overcome inhibitors in myelin and promote spinal axon regeneration in vivo. Neuron 2004;44:609–621. [PubMed: 15541310]
16. Geuna S, Papalia I, Tos P. End-to-side (terminolateral) nerve regeneration: a challenge for neuroscientists coming from an intriguing nerve repair concept. Brain Res Rev 2006;52:381–388. [PubMed: 16766038]
17. Gillingwater TH, Ribchester RR. Compartmental neurodegeneration and synaptic plasticity in the Wld(s) mutant mouse. J Physiol 2001;534:627–639. [PubMed: 11483696]
18. Gillingwater TH, Ribchester RR. The relationship of neuromuscular synapse elimination to synaptic degeneration and pathology: insights from WldS and other mutant mice. J Neurocytol 2003;32:863–881. [PubMed: 15034273]
19. Hayashi A, Koob JW, Liu DZ, Tong AY, Hunter DA, Parsadanian A, Mackinnon SE, Myckatyn TM. A double-transgenic mouse used to track migrating Schwann cells and regenerating axons following engraftment of injured nerves. Exp Neurol 2007;207:128–138. [PubMed: 17628544]
20. Hayashi A, Yanai A, Komuro Y, Nishida M, Inoue M, Seki T. Collateral sprouting occurs following end-to-side neurorrhaphy. Plast Reconstr Surg 2004;114:129–137. [PubMed: 15220580]
21. Hess JR, Myckatyn TM, Hunter DA, Mackinnon SE. Terminolateral fiber count. Plast Reconstr Surg 2005;116:1561–1562. [PubMed: 16217520]author reply 1562
22. Hunter DA, Moradzadeh A, Whitlock EL, Brenner MJ, Myckatyn TM, Wei CH, Tung TH, Mackinnon SE. Binary imaging analysis for comprehensive quantitative histomorphometry of peripheral nerve. J Neurosci Methods 2007;166:116–124. [PubMed: 17675163]
23. Iwase T, Jung CG, Bae H, Zhang M, Soliven B. Glial cell line-derived neurotrophic factor-induced signaling in Schwann cells. J Neurochem 2005;94:1488–1499. [PubMed: 16086701]
24. Keller-Peck CR, Feng G, Sanes JR, Yan Q, Lichtman JW, Snider WD. Glial cell line-derived neurotrophic factor administration in postnatal life results in motor unit enlargement and continuous synaptic remodeling at the neuromuscular junction. J Neurosci 2001;21:6136–6146. [PubMed: 11487637]

25. Keller-Peck CR, Walsh MK, Gan WB, Feng G, Sanes JR, Lichtman JW. Asynchronous synapse elimination in neonatal motor units: studies using GFP transgenic mice. Neuron 2001;31:381–394. [PubMed: 11516396]
26. Liu Y, Halloran MC. Central and peripheral axon branches from one neuron are guided differentially by Semaphorin3D and transient axonal glycoprotein-1. J Neurosci 2005;25:10556–10563. [PubMed: 16280593]
27. Lonze BE, Ginty DD. Function and regulation of CREB family transcription factors in the nervous system. Neuron 2002;35:605–623. [PubMed: 12194863]
28. Lundborg G, Zhao Q, Kanje M, Danielsen N, Kerns JM. Can sensory and motor collateral sprouting be induced from intact peripheral nerve by end-to-side anastomosis? Journal of Hand Surgery - British Volume 1994;19:277–282.
29. Mackinnon SE, Dellon AL, Hudson AR, Hunter DA. Chronic human nerve compression--a histological assessment. Neuropathology & Applied Neurobiology 1986;12:547–565. [PubMed: 3561691]
30. Magill CK, Tong A, Kawamura D, Hayashi A, Hunter DA, Parsadanian A, Mackinnon SE, Myckatyn TM. Reinnervation of the tibialis anterior following sciatic nerve crush injury: a confocal microscopic study in transgenic mice. Exp Neurol 2007;207:64–74. [PubMed: 17628540]
31. Matsumoto M, Hirata H, Nishiyama M, Morita A, Sasaki H, Uchida A. Schwann cells can induce collateral sprouting from intact axons: experimental study of end-to-side neurorrhaphy using a Y-chamber model. J Reconstr Microsurg 1999;15:281–286. [PubMed: 10363551]
32. Mennen U. End-to-side nerve suture in clinical practice. Hand Surg 2003;8:33–42. [PubMed: 12923932]
33. Mennen U, van der Westhuizen MJ, Eggers IM. Re-innervation of M. biceps by end-to-side nerve suture. Hand Surg 2003;8:25–31. [PubMed: 12923931]
34. Misgeld T, Nikic I, Kerschensteiner M. In vivo imaging of single axons in the mouse spinal cord. Nat Protoc 2007;2:263–268. [PubMed: 17406584]
35. Myckatyn TM, Mackinnon SE. The surgical management of facial nerve injury. Clin Plast Surg 2003;30:307–318. [PubMed: 12737358]
36. Myckatyn TM, MacKinnon SE. A review of research endeavors to optimize peripheral nerve reconstruction. Neurol Res 2004;26:124–138. [PubMed: 15072631]
37. Nichols CM, Myckatyn TM, Rickman SR, Fox IK, Hadlock T, Mackinnon SE. Choosing the correct functional assay: a comprehensive assessment of functional tests in the rat. Behav Brain Res 2005;163:143–158. [PubMed: 15979168]
38. Noah EM, Williams A, Fortes W, Terzis JK. A new animal model to investigate axonal sprouting after end-to-side neurorrhaphy. J Reconstr Microsurg 1997;13:317–325. [PubMed: 9258836]
39. Pan YA, Misgeld T, Lichtman JW, Sanes JR. Effects of neurotoxic and neuroprotective agents on peripheral nerve regeneration assayed by time-lapse imaging in vivo. J Neurosci 2003;23:11479–11488. [PubMed: 14673013]
40. Rafuse VF, Gordon T. Self-reinnervated cat medial gastrocnemius muscles. I. comparisons of the capacity for regenerating nerves to form enlarged motor units after extensive peripheral nerve injuries. J Neurophysiol 1996;75:268–281. [PubMed: 8822556]
41. Rafuse VF, Gordon T. Self-reinnervated cat medial gastrocnemius muscles. II. analysis of the mechanisms and significance of fiber type grouping in reinnervated muscles. J Neurophysiol 1996;75:282–297. [PubMed: 8822557]
42. Riccio A, Pierchala BA, Ciarallo CL, Ginty DD. An NGF-TrkA-mediated retrograde signal to transcription factor CREB in sympathetic neurons. Science 1997;277:1097–1100. [PubMed: 9262478]
43. Schafer M, Fruttiger M, Montag D, Schachner M, Martini R. Disruption of the gene for the myelin-associated glycoprotein improves axonal regrowth along myelin in C57BL/Wlds mice. Neuron 1996;16:1107–1113. [PubMed: 8663987]
44. Taveggia C, Zanazzi G, Petrylak A, Yano H, Rosenbluth J, Einheber S, Xu X, Esper RM, Loeb JA, Shrager P, Chao MV, Falls DL, Role L, Salzer JL. Neuregulin-1 type III determines the ensheathment fate of axons. Neuron 2005;47:681–694. [PubMed: 16129398]

45. Thanos PK, Tiangco DA, Terzis JK. Enhanced reinnervation of the paralyzed orbicularis oculi muscle after insulin-like growth factor-I (IGF-I) delivery to a nerve graft. J Reconstr Microsurg 2001;17:357–362. [PubMed: 11499470]

46. Viterbo F, Trindade JC, Hoshino K, Mazzoni Neto A. Latero-terminal neurorrhaphy without removal of the epineural sheath. Experimental study in rats. Rev Paul Med 1992;110:267–275. [PubMed: 1341024]

47. Watson FL, Heerssen HM, Bhattacharyya A, Klesse L, Lin MZ, Segal RA. Neurotrophins use the Erk5 pathway to mediate a retrograde survival response. Nat Neurosci 2001;4:981–988. [PubMed: 11544482]

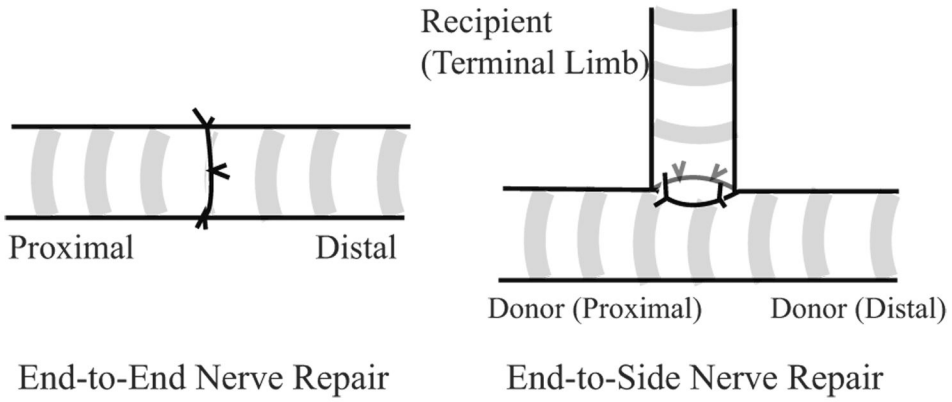

Figure 1.
In end-to-end repair, the transected nerve is reapproximated and secured with microsurgical technique. If the proximal stump is unavailable for end-to-end repair, one option is to coapt the recipient (terminal) limb of the distal transected nerve to the donor nerve in an end-to-side (ETS) fashion. The basal lamina tubes of the terminal limb remain structurally contiguous with motor endplates and sensory receptors.

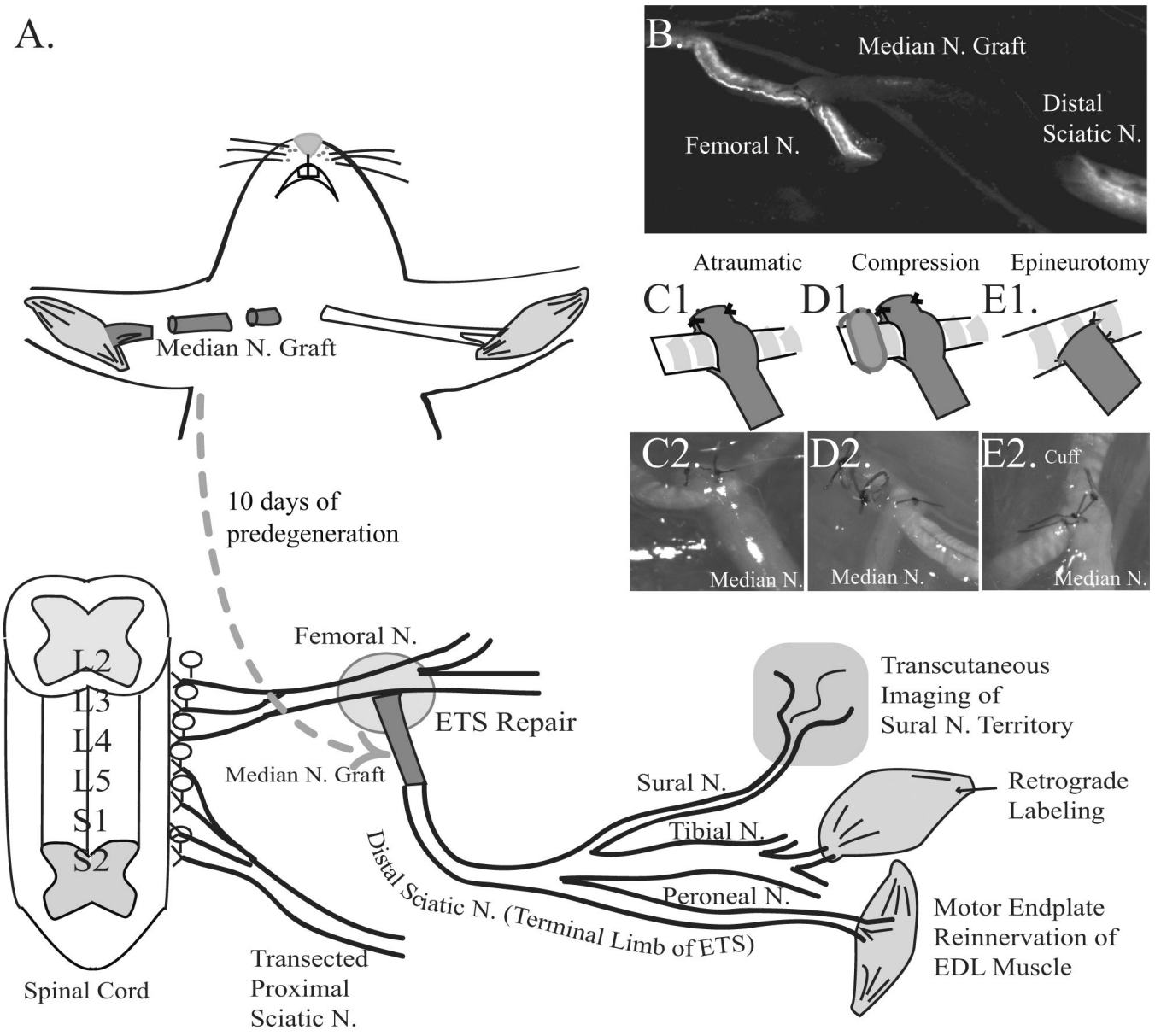

Figure 2. Schematic of experimental design

A. The median nerve was proximally transected 10 days prior to ETS repair to eliminate YFP- or GFP-labeled axons. The 5 mm median nerve graft was coapted ETS to the common femoral nerve proximally, and end-to-end into the distal stump of the transected sciatic nerve distally. Motor endplate reinnervation of extensor digitorum longus (EDL), retrograde labeling of the gastrocnemius muscle to the L2–L4 spinal cord, and cutaneous reinnervation of the sural nerve territory were evaluated. **B.** Live image at t=0, with a fluorescence naïve median nerve graft spanning the femoral nerve proximally, and the sciatic nerve distally in a mThy1-GFP(S) mouse. The labeled axons in the transected sciatic nerve also degenerated to facilitate axon tracking. **C1.** Schematic of “atraumatic” repair. **C2.** Brightfield image. **D1.** Schematic of “compression” repair. *D2.* Brightfield image. **E1.** Schematic of “epineurotomy”. **E2.** Brightfield image.

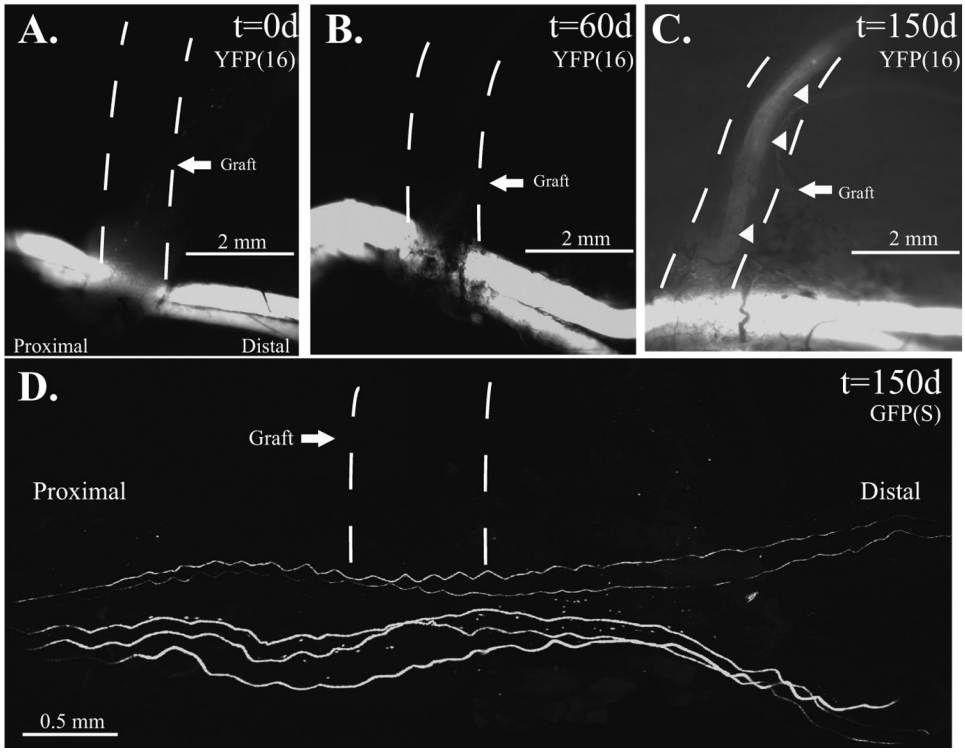

Figure 3. Atraumatic ETS repair

A. The fluorescent-naïve median nerve graft, marked by a dashed line, is sutured ETS to the donor common femoral nerve using the sleeve technique and imaged at t=0 days in a mThy1-YFP(16) mouse. **B.** No axons observed regenerating into the recipient limb at t=60 days in mThy1-YFP(16) mice. **C.** By 150 days, faint fluorescence is noted in 50% of mThy1-YFP(16) mice. **D.** In mThy1-GFP(S) mice, all of the grafts remained devoid of fluorescent-labeled axons to 150 days.

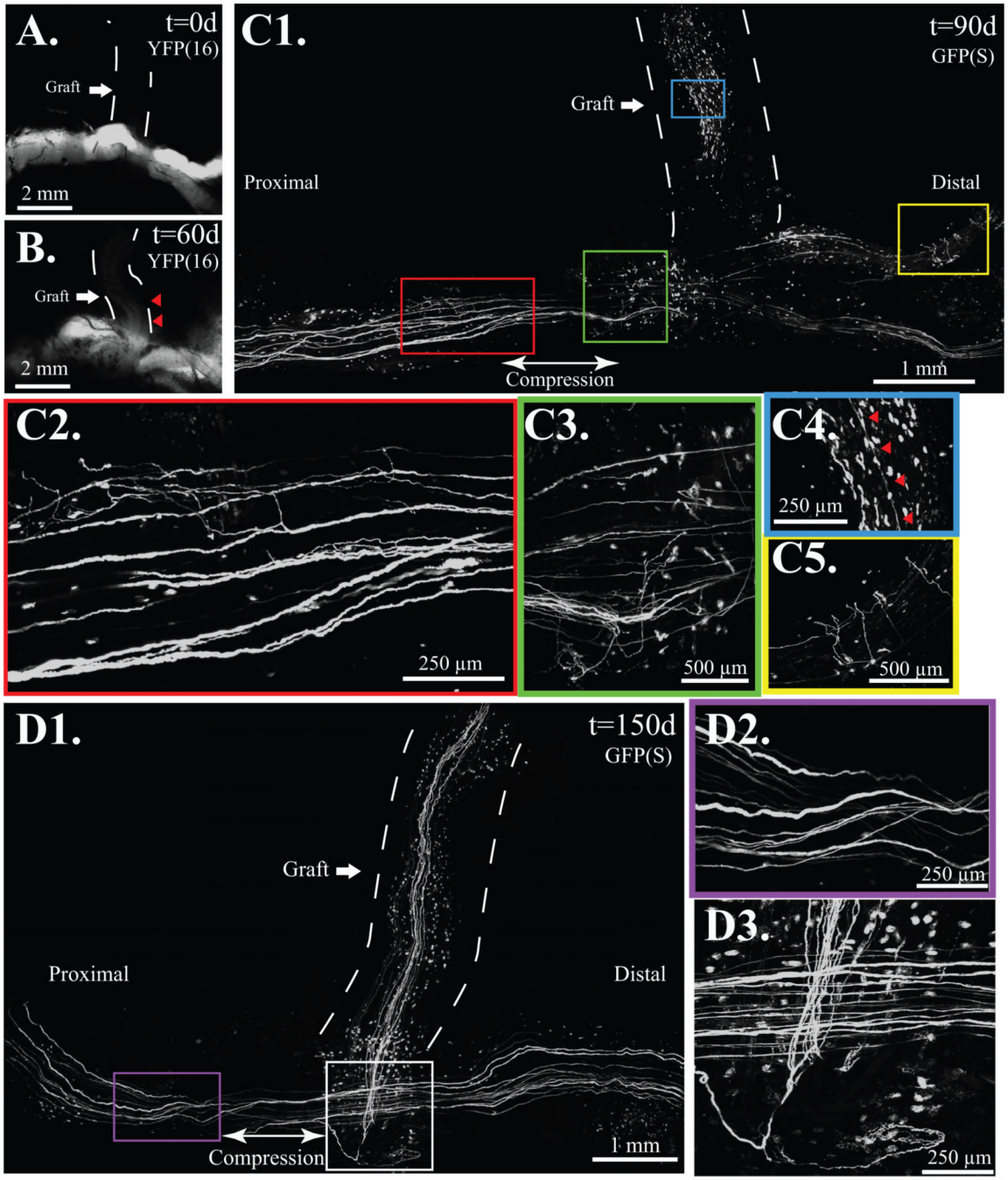

Figure 4. Compressive ETS repair resembles the atraumatic technique but with proximal compression

A. The fluorescent-naïve median nerve graft, marked is by a dashed line. **B.** At 60 days, axons are noted in the proximal graft marked by red arrows in mThy-YFP(16) mice. **C1.** By 90 days, regenerative sprouts, shown here under confocal microscopy on a fixed mThy1-GFP(S) specimen, were noted along the length of the donor nerve and recipient limbs. **C2.** Axonal sprouts proximal, **C3.** and distal to compression. **C4.** A few axons, marked by red arrows noted in the previously fluorescent naïve graft. **C5.** Multiple regenerative sprouts noted distal to the ETS repair. **D1.** Numerous graft-based axons noted by 150 days, **D2.** but proximal (shown

here) and distal sprouting, noted at 90 days, absent by 150 days. **D3.** Sprouts were confined to the region of ETS repair at 150 days.

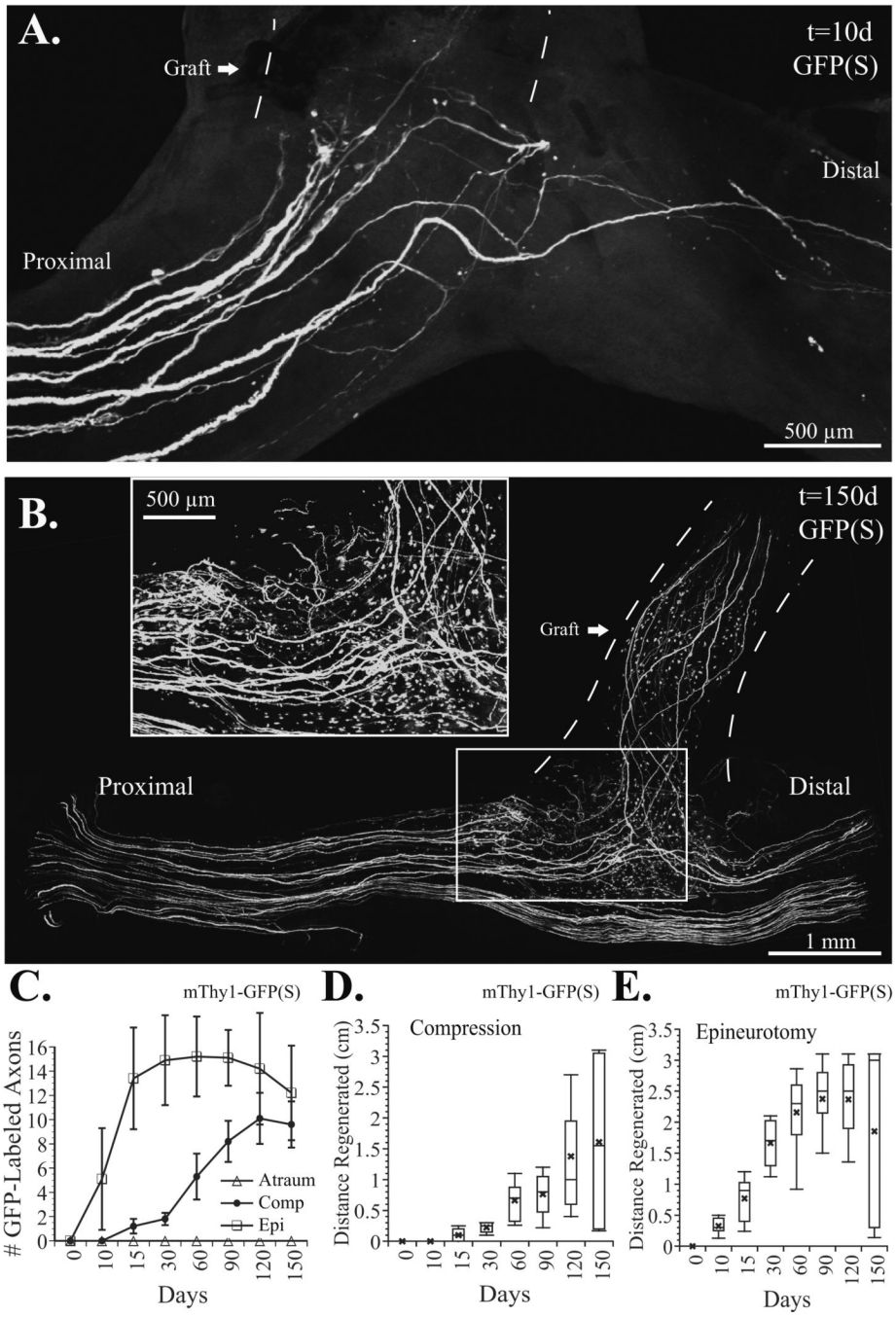

Figure 5.

A. Epineurotomy resulted in a clear disruption of axons distal to the repair and numerous regenerating units at 10 days. **B.** By 150 days, many axons noted in the recipient (graft) limb, and proportionately fewer axons noted in the distal than proximal donor nerve. Numerous sprouts still present, however (see inset). **C.** The few labeled motor axons entering the fluorescence naïve graft were counted from flattened z-stacks obtained in living mThy1-GFP (S) mice (≤10% of motor, few if any sensory axons labeled). No axons entered the traumatic repairs (open triangles), while a few axons were noted in the compression group within 10–15 days (filled circles), and in the epineurotomy group (squares) in ≤10 days. **D.** Box plots show the distance that axons penetrated the compressive ETS repair. Error bars represent the 10th

and 90th percentiles, while the top of the box represents the 75th percentile, the central line the 50th percentile (median), and the bottom of the box the 25th percentile. The "x" denotes the mean axon length. **E.** Box plot of the epineurotomy ETS repair shows a gradual increase in the median and mean axon length (the maximal distance to the motor endplates was ≤3.5 cm) to 120 days. By 150 days, however, the mean but not median axon length fell.

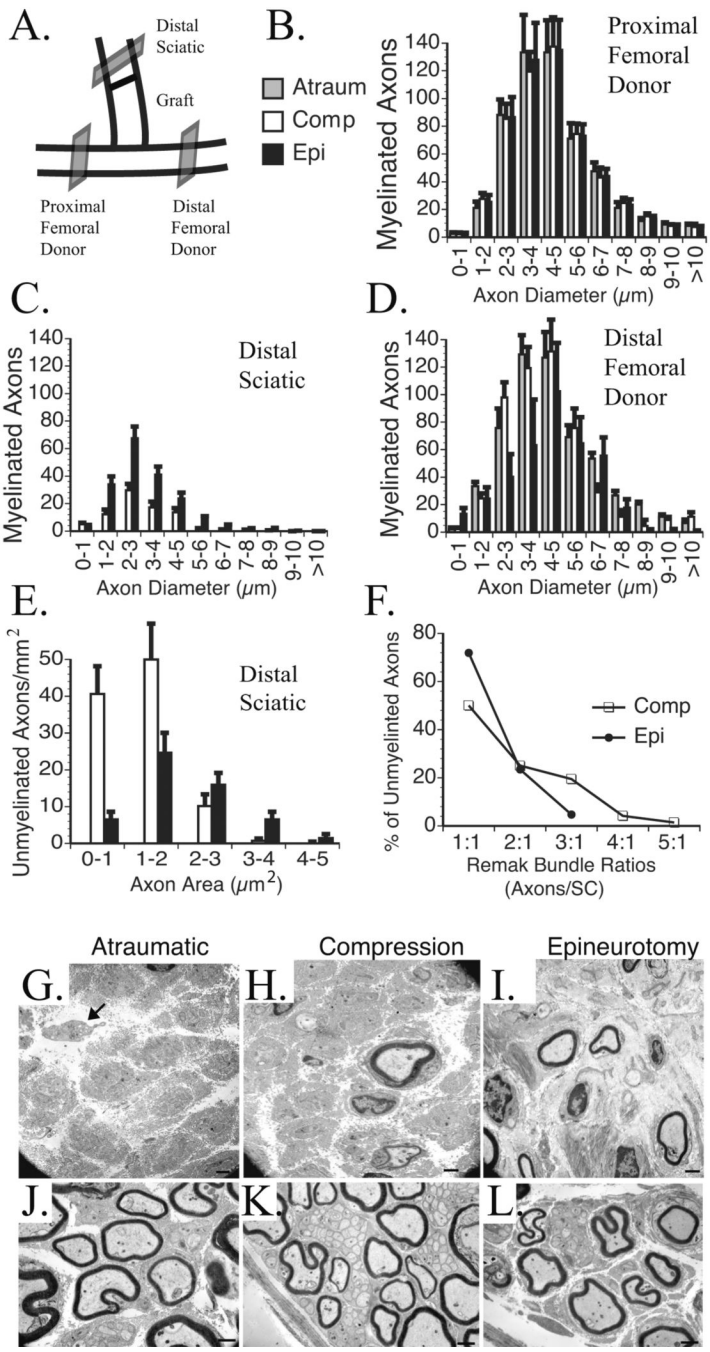

Figure 6. Morphometric and stereologic assessment of donor and recipient nerve cross sections

A. Donor nerves were sectioned 5 mm proximal and distal to the ETS repair and in the reconstructed limb of the transected sciatic nerve 5 mm distal to the median nerve graft. **B.** The proximal femoral donor nerve demonstrated a consistent distribution of myelinated axons counts based on fiber widths. **C.** The reconstructed sciatic nerve demonstrated the most axons with epineurotomy repair, and none with atraumatic repair. **D.** The distal femoral nerve demonstrated progressively fewer myelinated axons from atraumatic to compressive to epineurotomy ETS repair. **E.** Compressive repair resulted in the highest total number of unmyelinated axons, particularly with areas ≤2 μm^2. No unmyelinated axons were noted with the atraumatic repair. **F.** A higher percentage of unmyelinated axons were associated with

larger Remak bundles with compressive than epineurotomy repair. **G.** EM of sciatic nerve reconstructed with atraumatic; **H.** compressive; **I.** epineurotomy repair. Arrow points to scant unmyelinated axons that lack a double basement membrane or SCs. **J.** Distal femoral donor nerve reconstructed with atraumatic; **K.** compressive; **L.** epineurotomy ETS repair. In compressive repair (**K.**), note the particularly large Remak bundles with up to 47 unmyelinated axons per SC distal to the compressive ETS repair. Scale bars 1 μm.

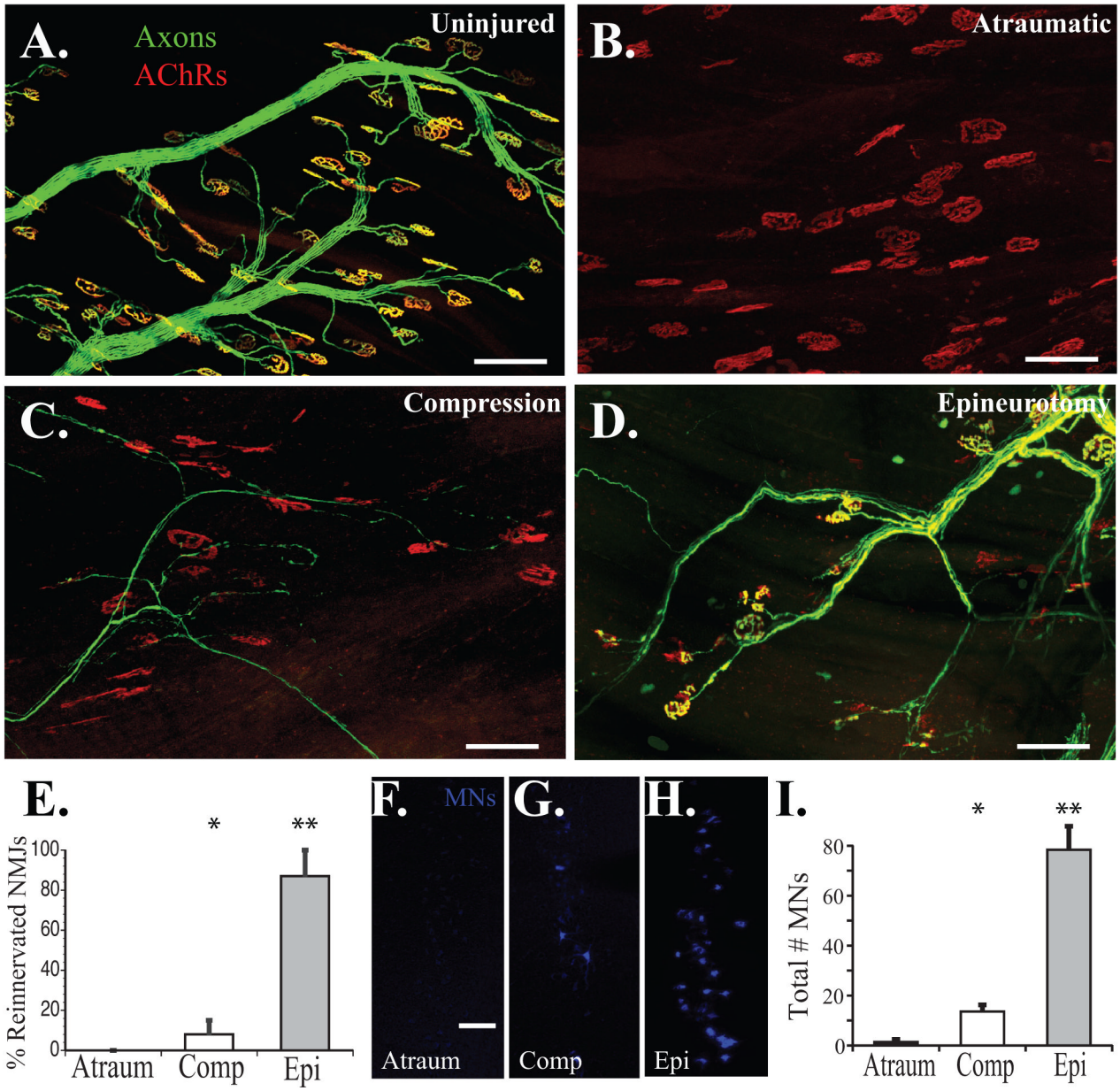

Figure 7. Quantification of motor target reinnervation at 150 days

A. Uninjured EDL muscle demonstrates 100% motor endplate innervation. **B.** No endplate reinnervation was observed with atraumatic ETS repairs. **C.** A few motor endplates were reinnervated with compressive repair. **D.** The majority of remaining motor endplates were reinnervated with epineurotomy repair. **E.** Quantification of motor endplate reinnervation with atraumatic (Atraum), compression (Comp), and epineurotomy (Epi) ETS repairs. **F.** Retrograde-labeled femoral nerve ventral MNs at the L2-L4 spinal cord level in the atraumatic, **G.** compressive, and **H.** and epineurotomy ETS repairs. The femoral nerve now innervated the gastrocnemius, which was previouly innervated by the tibial nerve (S1–S2). **I.** Epineurotomy resulted in a significantly higher number of retrograde labeled ventral MNs originating at the L2–L4 levels, while atraumatic repair demonstrated occasional background, but statistically insignificant labeling (* $p<0.05$; ** $p<0.0001$). Scale bars 100 μm.

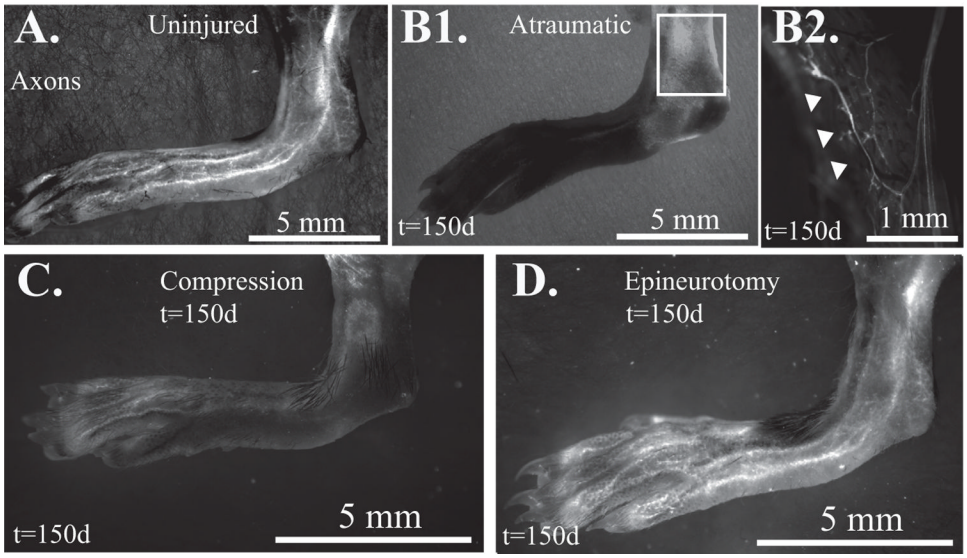

Figure 8. Transcutaneous imaging of the sural nerve

A. Uninjured control shows sural nerve appearing inferior to the hamstring and innervating the lateral lower leg, ankle, and skin over the dorsal fifth metatarsal of the foot. **B1.** With atraumatic ETS repair, no sciatic nerve branches are visualized at 150 days at low magnification. **B2.** At higher resolution, a few YFP-labeled cutaneous axons (white arrowheads) were noted, in one mouse in the sural nerve territory. **C.** Scant reinnervation of a few peroneal branches on the dorsum of the foot, but no clear sural nerve branches with compressive ETS repair. **D.** Restoration of sural nerve (and visible peroneal nerve) with epineurotomy repair by 150 days.

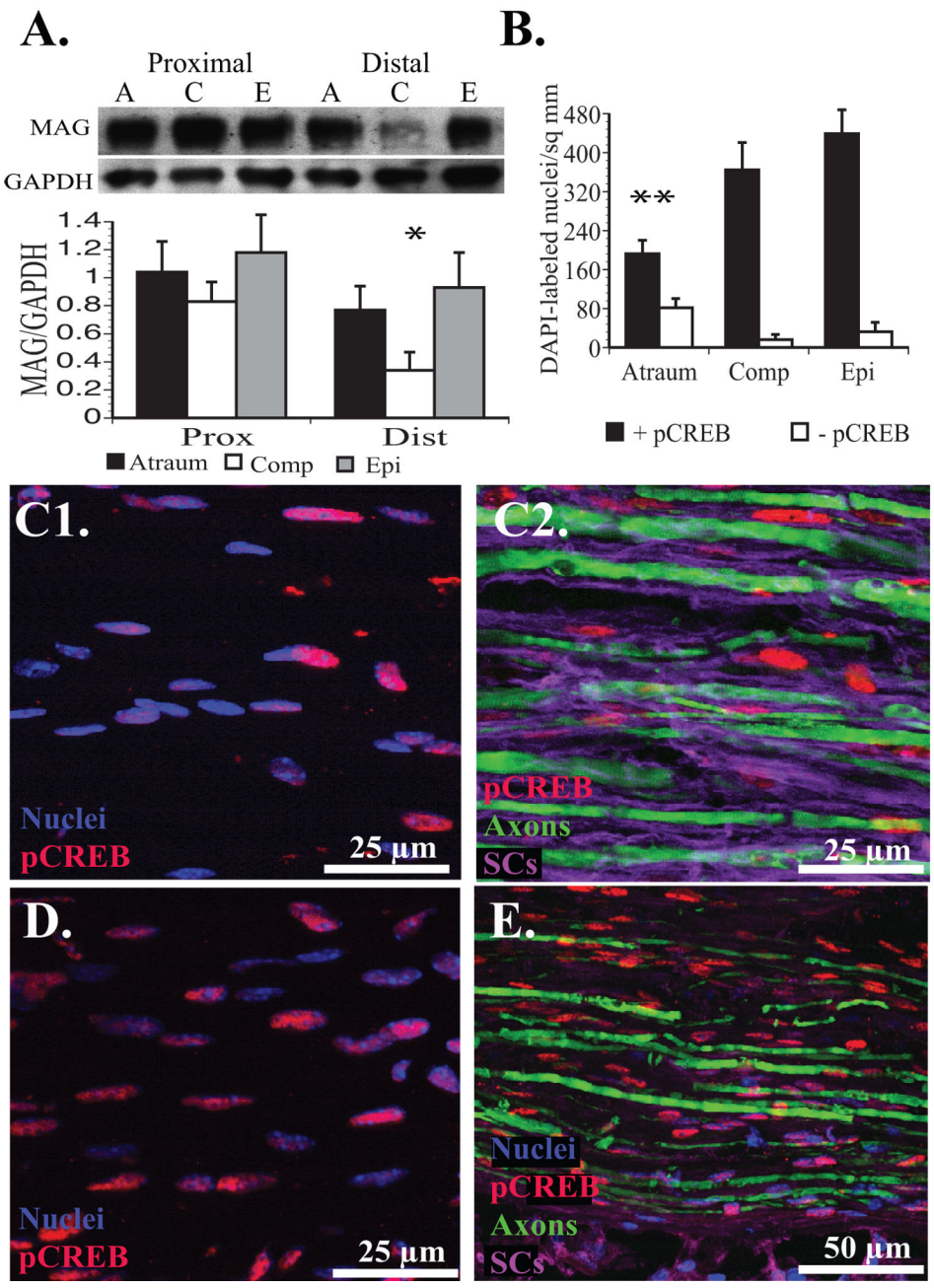

Figure 9. Assessment of MAG expression and CREB phosphorylation 21 days after ETS repair

A. MAG expression was significantly downregulated in the compression group distal to the cuff and ETS repair site when normalized to GAPDH signal (* $p<0.05$). **B.** The number of nuclei with and without strong pCREB expression within the donor nerve immediately distal to the ETS repair. There were significantly fewer nuclei overall with relatively less pCREB expression in the atraumatic repair (** $p<0.01$) compared to all other groups. **C1.** Moderate colabeling in an atraumatic repair. **C2.** pCREB appears to colocalize with SCs (purple) enveloping axons (green). **D.** With proximal compression, a much higher percentage of nuclei express pCREB. **E.** With epineurotomy, pCREB also colocalizes with SCs surrounding axons.